Structural and Magnetic Characterization of the Series $La_{1-x}Sr_xFe_{0.8}Cr_{0.2}O_{3-\delta}$ ($x = 0.2$, 0.4, 0.6, and 0.8)

T. Ramos*

CCMM, Faculdade de Ciências, Universidade de Lisboa, 1749-016 Lisboa, Portugal

M. D. Carvalho

CCMM/Dep. Química e Bioquímica, Faculdade de Ciências, Universidade de Lisboa, 1749-016 Lisboa, Portugal

L. P. Ferreira

CFMC, Faculdade de Ciências, Universidade de Lisboa, 1749-016 Lisboa, Portugal and Dep. Física, Faculdade de Ciências e Tecnologia, Universidade de Coimbra, 3004-516 Coimbra, Portugal

M. M. Cruz and M. Godinho

CFMC/Dep. Física, Faculdade de Ciências, Universidade de Lisboa, 1749-016 Lisboa, Portugal

Received March 22, 2006. Revised Manuscript Received May 29, 2006

A series of perovskite compounds with the general formula $La_{1-x}Sr_xFe_{0.8}Cr_{0.2}O_{3-\delta}$ ($x = 0.2$, 0.4, 0.6, and 0.8) have been synthesized using a urea/nitrates self-combustion route. Their characterization was performed using room-temperature X-ray diffraction, electrical and magnetization measurements. A structural transition from orthorhombic ($x = 0.2$) to rhombohedral ($x > 0.2$) was determined. Among the rhombohedral phases, increased Sr content caused a visible decrease in distortion. Monotonic decreases with increasing x were found for both the pseudocubic lattice parameter (a') and <Fe/Cr−O> bond lengths in the $0.2 \leq x \leq 0.6$ range, which have been attributed to an increase in the mean oxidation state of the transition metals. The lattice expansion observed for $x = 0.8$, in addition to an apparent stabilization of the <Fe/Cr−O> bond lengths for $x = 0.6$ and 0.8, suggested an increased role for oxygen vacancy formation as the charge compensation regime for the latter. All compounds exhibited semiconductor behavior with temperature dependencies better described by the 3d variable range hopping model. The monotonic decrease of resistivity with increasing x in the $0.2 \leq x \leq 0.6$ range was found consistent with an increase in carrier density. The monotony is broken for $x = 0.8$, which was also associated with the change in the charge compensation regime. Increased x progressively weakened the overall antiparallel coupling of the magnetic moments, inducing a decrease of the ordering temperature for samples in the $0.2 \leq x \leq 0.8$ range.

Introduction

Over the past decades, there has been a continued interest in the development of new materials with the perovskite structure. The framework of ABO_3 perovskite oxides is the corner-linked BO_6 octahedra, having the larger A cation in a 12-coordinated site. It has been established that the existence of mixed valence states on the B-site (e.g., transition metals) plays an essential role in determining the physical properties of such oxides.[1] In addition, structural changes introduced by doping also play a crucial role, as they extend throughout the lattice affecting both the B−O bond lengths and B−O−B bond angles.[2] The influence of the crystal structure and the valence of the transition metals of these perovskite-type oxides on their properties cannot be disregarded, and further understanding of this relation is crucial if we are to predict and tailor behaviors.

Perovskite compounds have been envisaged as mixed ionic electronic conductors (MIECs) for application as fuel cell electrodes, pressure-driven oxygen separators, and particularly as membranes for the partial oxidation of light hydrocarbons. For these applications, the requirement of stable compounds under reducing conditions demonstrated that perovskite phases containing iron and chromium are promising materials.[3,4]

In previous works, compositions in the $La_{1-x}Sr_xFe_{0.8}Cr_{0.2}O_{3-\delta}$ series were proposed as suitable materials for dense membranes in methane reformers and chemical reactors. However, further understanding of the structural influence on the physical properties was necessary.[5−7]

* To whom correspondence should be addressed. Phone: (351) 21 750 0075. Fax: (351) 21 750 0088. E-mail: tmramos@fc.ul.pt.

(1) Peña, M. A.; Fierro, J. L. G. *Chem. Rev.* **2001**, *101*, 1981.
(2) Pandey, S. K.; Bindu, R.; Bhatt, P.; Chaudhari, S. M.; Pimpale, A. V. *Physica B* **2005**, *365*, 47.
(3) Nakamura, T.; Petzow, G.; Gauckler, L. G. *Mater. Res. Bull.* **1979**, *14*, 649.
(4) Mizusaki, J.; Mima, Y.; Yamauchi, S.; Fueki, K.; Tagawa, H. *J. Solid State Chem.* **1989**, *80*, 102.
(5) Ramos, T.; Atkinson, A. *Solid State Ionics* **2004**, *170*, 275.

10.1021/cm060689s CCC: $33.50
Published on Web 07/04/2006

The present work aims to contribute to a further understanding of the structural characteristics that govern the exhibited properties of $La_{1-x}Sr_xFe_{0.8}Cr_{0.2}O_{3-\delta}$ ($x = 0.2$, 0.4, 0.6, and 0.8) phases, which were characterized using room-temperature X-ray powder diffraction, electrical and magnetization measurements.

Experimental Section

Ceramic powders of $La_{1-x}Sr_xFe_{0.8}Cr_{0.2}O_{3-\delta}$ with nominal compositions $x = 0.2$, 0.4, 0.6, and 0.8 were prepared by a urea/nitrate self-combustion route. The starting metal oxides, carbonates, or oxalates of reagent grade were mixed in the appropriate molar ratios and then dissolved in nitric acid. The obtained solution was then mixed with urea and heated until a concentrated gel was formed. Further heating autoignited the gel into a vigorous and rapid combustion. The resulting powder was calcined at 873 K/6 h, to remove any remaining organics, before being further calcined in air at temperatures ranging from 1273 to 1623 K, with intermediate grinding, until the desired phase was obtained, as confirmed by X-ray powder diffraction (XRD).

Structural characterization by room-temperature XRD was performed using a Philips PW 1730 powder diffractometer, operating with a Cu Kα radiation and previously calibrated using a Si standard. The XRD patterns were obtained for 2θ between 20° and 120° in steps of 0.02° and analyzed by Rietveld refinement using the FullProf program.[8] A polynomial function was used to model the background level. Peak shapes were fitted using a pseudo-Voigt function and two asymmetry parameters. A preferred orientation correction was included in the different refinements, and the occupation factors were fixed taking into account sample stoichiometry, assuming that all oxygen sites were fully occupied.

Electrical resistivity was measured between 10 and 300 K using a standard four-point probe technique for a constant current of 10 μA.

Magnetization measurements as a function of temperature (M−T) and as a function of the applied magnetic field (M−H) were performed using a SQUID magnetometer (Quantum Design MPMS). The M−T curves were obtained at different magnetic fields (0.005−0.5 T) for temperatures ranging from 2 to 350 K. Data were collected in increasing temperature after both zero-field cooling (ZFC) and field cooling (FC). The isothermal M−H curves were measured for magnetic fields up to 5.5 T.

Results and Discussion

The XRD patterns of the $La_{1-x}Sr_xFe_{0.8}Cr_{0.2}O_{3-\delta}$ ($x = 0.2$, 0.4, 0.6, and 0.8) revealed that the samples consisted mainly of the perovskite phase. An extra peak of small intensity (<0.3%) at $2\theta \cong 29.4°$ appeared for all studied compositions. This peak was excluded from each structural refinement. The analysis of these results by the Rietveld method was initially based on previous results for the similar materials $La_{1-x}Sr_xFeO_{3-\delta}$[9] and $La_{1-x}Sr_xFe_{0.8}Co_{0.2}O_{3-\delta}$,[10] which indicated three different crystallographic regions when $\delta \cong 0$: orthorhombic (*Pnma* space group) for $0 \le x \le 0.2$, rhombohedral ($R\bar{3}c$ space group) for $0.4 \le x \le 0.7$, and cubic ($Pm\bar{3}m$ space group) for $x > 0.7$. However, in the present study and for the sample with nominal composition $x = 0.8$, a reflection at $2\theta \cong 38.4°$, forbidden for the $Pm\bar{3}m$ symmetry, indicates a possible distortion from the ideal cubic structure. As a consequence, the rhombohedral space group $R\bar{3}c$ was also tested. This refinement resulted in a significant improvement of the conventional agreement factors, namely, on the R_{Bragg} (from 4.22 in the $Pm\bar{3}m$ space group, excluding the forbidden reflection, to 3.64 in the $R\bar{3}c$ space group). The rhombohedral symmetry was thus chosen for the $x = 0.8$ sample.

Figure 1 shows the experimental and calculated XRD patterns for all compositions. Tables 1−3 present the crystallographic information obtained from the refinements, in addition to other relevant parameters. Table 4 presents the relevant results obtained for bond lengths and angles, for all compositions.

The structural results can be firstly analyzed considering that the primary effect is due to the substitution of lanthanum by strontium. As the larger Sr^{2+} substitutes La^{3+} ions ($r(La^{3+})_{XII} = 1.36$ Å, $r(Sr^{2+})_{XII} = 1.44$ Å),[11] both the average ionic radius for A ions ($<r_A>$) and the tolerance factor (t) are increased (Table 5). The structural transformation from a highly distorted orthorhombic structure ($x = 0.2$) to a gradually less distorted rhombohedral symmetry ($x \ge 0.4$) is in accordance with the calculated tolerance factor values. These results are also in good agreement with the trend shown by $A^{3+}B^{3+}O_3$ perovskites, as they suffer a transition from rhombohedral to orthorhombic symmetry with decreasing r_A/r_B ratio.[12]

Figure 2 illustrates the effect of Sr doping on the pseudocubic lattice constant (a'), which corresponds to the calculated cube root of the unit cell volume per ABO_3, relating both (x and a') with the (Fe/Cr)−O−(Fe/Cr) bond angle (upper figure) and <(Fe/Cr)−O> bond length (lower figure). Among the rhombohedral phases, a visible decrease in distortion with increasing Sr content can be inferred by the increase in the (Fe/Cr)−O−(Fe/Cr) angle, which gradually approaches the ideal 180° as we move from $x = 0.4$ to $x = 0.8$. The less distorted structure for $x = 0.8$ can explain why simpler XRD analysis could infer a cubic symmetry for this solid solution. The present results are in good agreement with those reported for $SrFe_{1-x}Cr_xO_{3-y}$.[13] In the present study, when $0.2 \le x \le 0.6$, a' decreases with increasing x. It seems clear that, in this compositional range, substituting La^{3+} with a lower valence cation induces a lattice contraction. A different behavior is observed for sample with $x = 0.8$ as the lattice clearly expands, when compared to that with $x = 0.6$. If the charge compensation induced by Sr doping on the A-site is primarily achieved by oxidation of the transition metals, increasing concentrations of Fe/Cr in higher oxidation states progressively decrease $<r_B>$ and strengthen the (Fe/Cr)−O bond. This results in a monotonic <(Fe/Cr)−O> bond length dependence on x. Increasing amounts of Sr progressively shorten the <(Fe/Cr)−O> bond

(6) Atkinson, A.; Ramos, T. *J. Power Sources* **2004**, *130*, 129.
(7) Ramos, T. Ph.D. Thesis, University of London, 2003.
(8) Roisnel, T.; Rodriguez-Carvajal, J. *FullProf Suite*, April 2005. Available on the internet: http:/www.llb.cea.fr.
(9) Dann, S. E.; Currie, D. B.; Weller, M. T.; Thomas, M. F.; Al-Rawwas, A. D. *J. Solid State Chem.* **1994**, *109*, 134.
(10) Tai, L.-W.; Nasrallah, M. M.; Anderson, H. U.; Sparlin, D. M.; Sehlin, S. R. *Solid State Ionics* **1995**, *76*, 273.
(11) Shannon, R. D. *Acta Crystallogr.* **1976**, *A32*, 751.
(12) Thomas, N. W. *Br. Ceram. Trans.* **1997**, *96*, 7.
(13) MacChesney, J. B.; Potter, J. F.; Sherwood, R. C. *J. Appl. Phys.* **1969**, *40*, 1243.

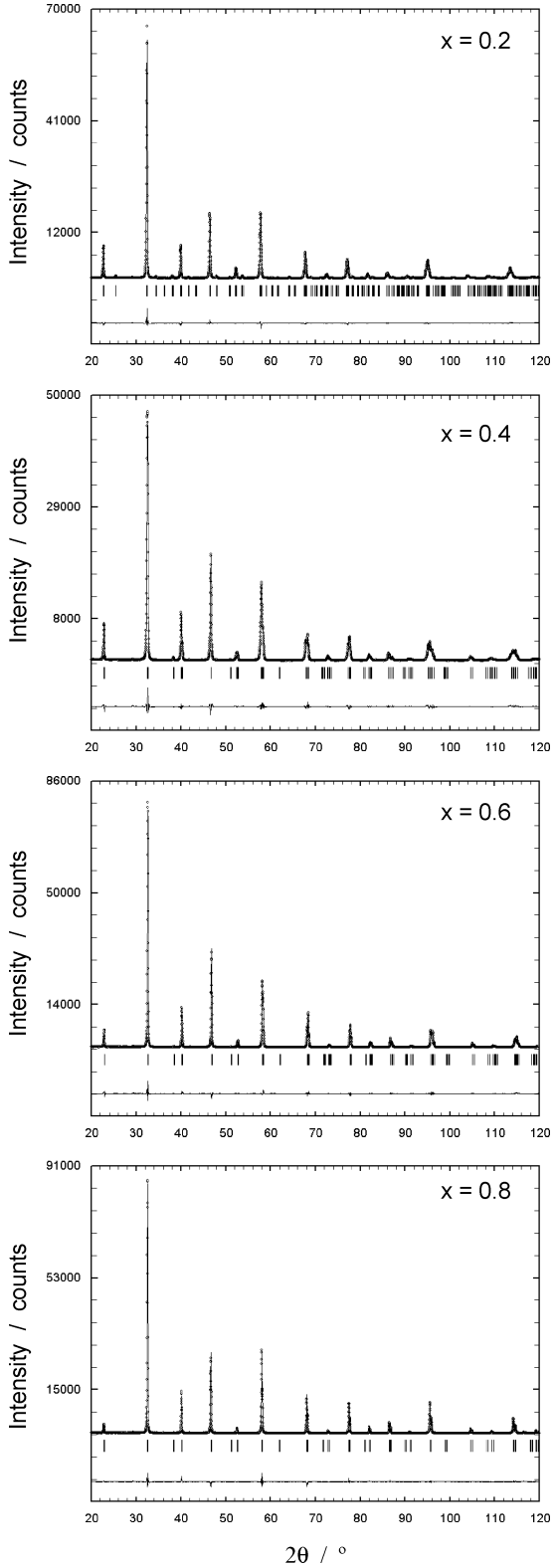

Figure 1. Observed (points) and calculated (solid line) Rietveld refinement plots of the XRD patterns of the $La_{1-x}Sr_xFe_{0.8}Cr_{0.2}O_{3-\delta}$ phases. The difference between observed and calculated is shown at the bottom of each pattern. Tick marks represent allowed reflections.

length, with subsequent lattice contraction. As can be seen in Figure 2, when $0.2 \leq x \leq 0.6$, both a' and <(Fe/Cr)−O> decrease with increasing x in an approximately linear relationship. This is a clear indication that, in the compositional range of $0.2 \leq x \leq 0.6$, Fe/Cr oxidation is the preferred charge compensation regime, simultaneously suggesting that

Table 1. Cell Parameters Values of the $La_{1-x}Sr_xFe_{0.8}Cr_{0.2}O_{3-\delta}$ Phases

		cell parameters		
x	vol/Å^3	*a*/Å	*b*/Å	*c*/Å
0.2	239.10(1)	5.5212(1)	7.8080(2)	5.5464(1)
0.4	354.02(2)	5.5200(1)		13.416(3)
0.6	350.93(1)	5.4973(1)		13.4088(2)
0.8	353.86(2)	5.5057(1)		13.4796(6)

Table 2. Structural Parameters of the $La_{0.8}Sr_{0.2}Fe_{0.8}Cr_{0.2}O_{3-\delta}$ Phase (Space Group: *Pnma*)[a]

		atomic positions		
atom	site	x	y	z
La/Sr	4*c*	0.0174(1)	0.25	−0.0042(2)
Fe/Cr	4*b*	0	0	0.5
O (1)	8*d*	0.265(1)	0.0261(8)	0.723(1)
O (2)	4*c*	0.495(1)	0.25	0.075(2)

[a] Conventional agreement factors: $R_{wp} = 8.16\%$, $R_p = 6.31\%$, and $R_{Bragg} = 2.92$.

Table 3. Structural Parameters of the $La_{1-x}Sr_xFe_{0.8}Cr_{0.2}O_{3-\delta}$ Phases (Space Group: $R\bar{3}c$; La/Sr (*6a*) (0 0 1/4); Fe/Cr (*6b*) (0 0 0); O (18e) (*x* 0 1/4)) and Conventional Agreement Factors

	x = 0.4	*x* = 0.6	*x* = 0.8
O (18e) *x*	0.5422(5)	0.529(1)	0.508(2)
R_{wp} (%)	9.77	8.43	9.40
R_p (%)	7.80	6.85	7.68
R_{Bragg}	2.28	2.55	3.64

Table 4. Selected Bond Lengths (Å) and Angles (°) for the $La_{1-x}Sr_xFe_{0.8}Cr_{0.2}O_{3-\delta}$ Phases

x	Fe/Cr−O/Å	Fe/Cr−O−Fe/Cr/°
0.2	M−O(1): 2.019(6)	M−O(1)−M: 164.7(3)
	M−O(1): 1.929(7)	
	M−O(2): 1.996(2)	M−O(2)−M: 155.9(1)
	<Fe/Cr−O>: 1.981	
0.4	1.960(1)	166.4(1)
0.6	1.948(1)	170.2(1)
0.8	1.947(1)	177.4(1)

Table 5. Calculated Average A-Site Cation Radius (<r_A>) and Tolerance Factor ($t = (r_O + <r_A>)/\sqrt{2}(r_O + <r_B>)$) as a Function of Sr Content (*x*) for $La_{1-x}Sr_xFe_{0.8}Cr_{0.2}O_{3-\delta}$ Phases ($r(O^{2-}) = 1.40$ Å, $r(Fe^{3+}) = 0.645$ Å, $r(Cr^{3+}) = 0.615$ Å, and <r_B> = 0.639 Å)

x	<r_A>	t
0.0	1.36	0.957
0.2	1.376	0.963
0.4	1.392	0.968
0.6	1.408	0.974
0.8	1.424	0.979
1.0	1.44	0.985

no major oxygen deficiency should be found in this range. The increase seen in a' as x increases from 0.6 to 0.8 is accompanied by an apparent stabilization of the <(Fe/Cr)−O> bond length, thus <r_B>. In view of this behavior, and taking into account that oxygen vacancies cause the lattice to expand, it is reasonable to assume that, from $x = 0.6$ to $x = 0.8$, the formation of oxygen vacancies becomes the preferred charge compensation regime, over Fe/Cr oxidation. These results are in good agreement with results obtained for $La_{1-x}Sr_xFeO_{3-\delta}$ where, for $x \geq 0.7$, deviations to the ideal oxygen stoichiometry have been found.[14] Attempts to indirectly determine the room-temperature oxygen content of each sample were unsuccessful due to sample dissolution

(14) Banks, E.; Mizushima, M. *J. Appl. Phys.* **1969**, *40*, 1408.

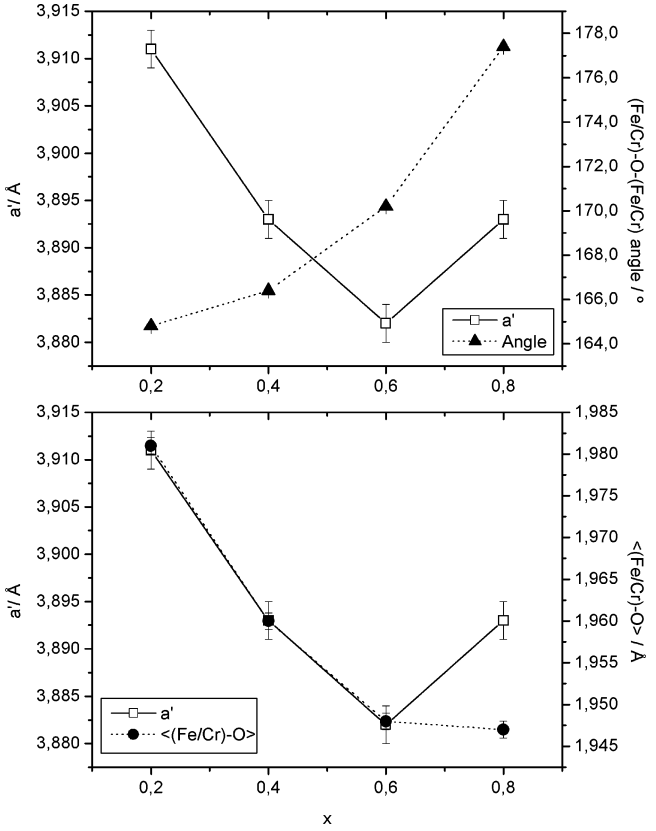

Figure 2. Variation of the pseudocubic lattice constant (a') with Sr doping and their relation to both (Fe/Cr)−O−(Fe/Cr) bond angles (upper figure) and <(Fe/Cr)−O> bond lengths (lower figure). Depicted lines are visual aids.

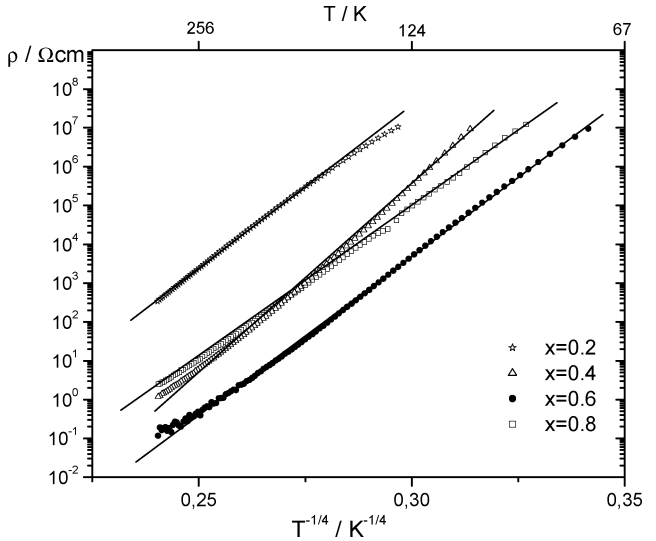

Figure 3. Electrical resistivity plotted as a function of $T^{-1/4}$ to display the 3d variable range hopping behavior.

problems (iodometric titrations) and enhanced chemical stability to reduction (thermogravimetry).

As to the electrical resistivity results, all compounds display a semiconductor-like behavior, attaining resistivity values higher than our experimental limit for low temperatures, below 120 K, depending on x. The corresponding temperature dependence cannot be explained by polaron hopping, and it is better described using a 3d variable range hopping (VHR), as shown in Figure 3, where the results are plotted in a logarithmic scale as a function of $T^{-1/4}$. A

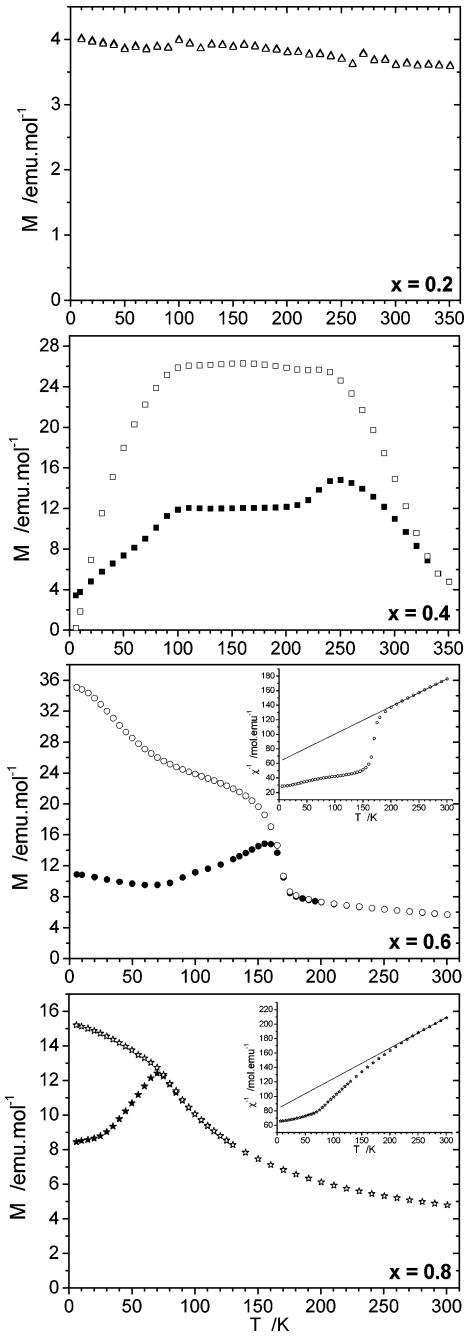

Figure 4. Magnetization as a function of temperature measured under 0.1 T for $La_{1-x}Sr_xFe_{0.8}Cr_{0.2}O_{3-\delta}$ (ZFC curves, closed symbols; FC curves, open symbols). The two insets correspond to the inverse of the magnetic susceptibility as a function of the temperature for $x = 0.6$ and 0.8.

monotonic decrease with increasing Sr content was measured for $0.2 \leq x \leq 0.6$, in agreement with an increase of carrier density induced by doping. For the $x = 0.8$ sample, the electrical resistivity is higher than the one for $x = 0.6$, indicating a different effect of Sr doping in the electrical conduction. This result agrees with a modification of the charge compensation mechanism for $x = 0.8$.

Figure 4 presents the M−T curves collected at 0.1 T for all samples. The transition temperatures to the ordered magnetic states (T_{ord}) for $0.4 \leq x \leq 0.8$, correspond to the temperatures at which the ZFC and FC curves split up (Table 6). As can be seen in Table 6, T_{ord} decreases as the Sr content increases, indicating weaker magnetic interactions for the compounds with higher Sr content. The M−T curves also

Table 6. Transition Temperatures to the Ordered Magnetic States (T_{ord}) Extracted from the M−T Curves for $x = 0.4$, 0.6, and 0.8 or Measured with a Vibrating Sample Magnetometer over the Temperature Range of 300−750 K under 0.1 T for $x = 0.2$

Sr content x	T_{ord} (K)
0.2	560(5)[a]
0.4	345(5)
0.6	170(5)
0.8	75(5)

[a] Ref 15.

show the signature of a different magnetic state at low temperatures, well defined for samples with $x = 0.4$ and 0.6. For the $x = 0.2$ compound the magnetization does not change significantly with temperature below 350 K, and the linear behavior of the M−H results measured at 35 and 300 K (not shown) indicates an antiparallel coupling of the magnetic moments, in agreement with the fact that Fe^{3+} and Cr^{3+} are expected to be the predominant valence ions and that $Cr^{3+}-O-Cr^{3+}$ as well as $Fe^{3+}-O-Fe^{3+}$ interactions are of the antiferromagnetic type. In fact, both $LaCrO_3$ and $LaFeO_3$ are antiferromagnetic materials with Néel temperatures of ~280 and 750 K, respectively.[16] In the substituted sample a ferromagnetic component due to the $Fe^{3+}(d^5)-O-Cr^{3+}(d^3)$ interaction was expected, although not observed. However, it was previously reported[17] that this effect would be observed only if the bond angle at the intervening anion was sufficiently close to 180°, which is not the present case (Table 4). A similar explanation was given for the results obtained for the $Ca_2Cr_{0.5}Fe_{1.5}O_5$ brownmillerite phase.[18]

Figure 5 presents some of the M−H curves measured for the samples with $0.4 \leq x \leq 0.8$. From the shape of the curves for temperatures below T_{ord}, an overall antiparallel coupling of the magnetic moments can also be inferred, as in the case of $x = 0.2$. For samples with $x = 0.4$ and 0.6, a small ferromagnetic component can be observed in some M−H curves. As previously mentioned, for $0.2 \leq x \leq 0.6$ the Fe/Cr oxidation seems to be the preferred charge compensation regime for Sr doping. Therefore, for $x \geq 0.4$, a significant number of cations are expected to be on higher oxidation states, namely, Fe^{4+}, Cr^{4+} and/or Cr^{6+}. Their increased presence would break the long-range magnetic order, which is consistent with the monotonic decrease found for T_{ord} with increased x, but could also justify the small ferromagnetic component due to parallel interactions induced by the presence of Fe^{4+} and Cr^{4+} ions. The competition between the different coexisting antiferromagnetic and ferromagnetic interactions can explain the modifications of the magnetic state detected at low temperatures in the M−T curves. This low temperature state is attributed to the existence of frustration that prevails at low fields and fades away at higher applied fields as observed in the M−H curves when $x \geq 0.4$. For the $x = 0.4$ compound, the competition leads to the reentrant behavior observed (Figure 4), with an almost

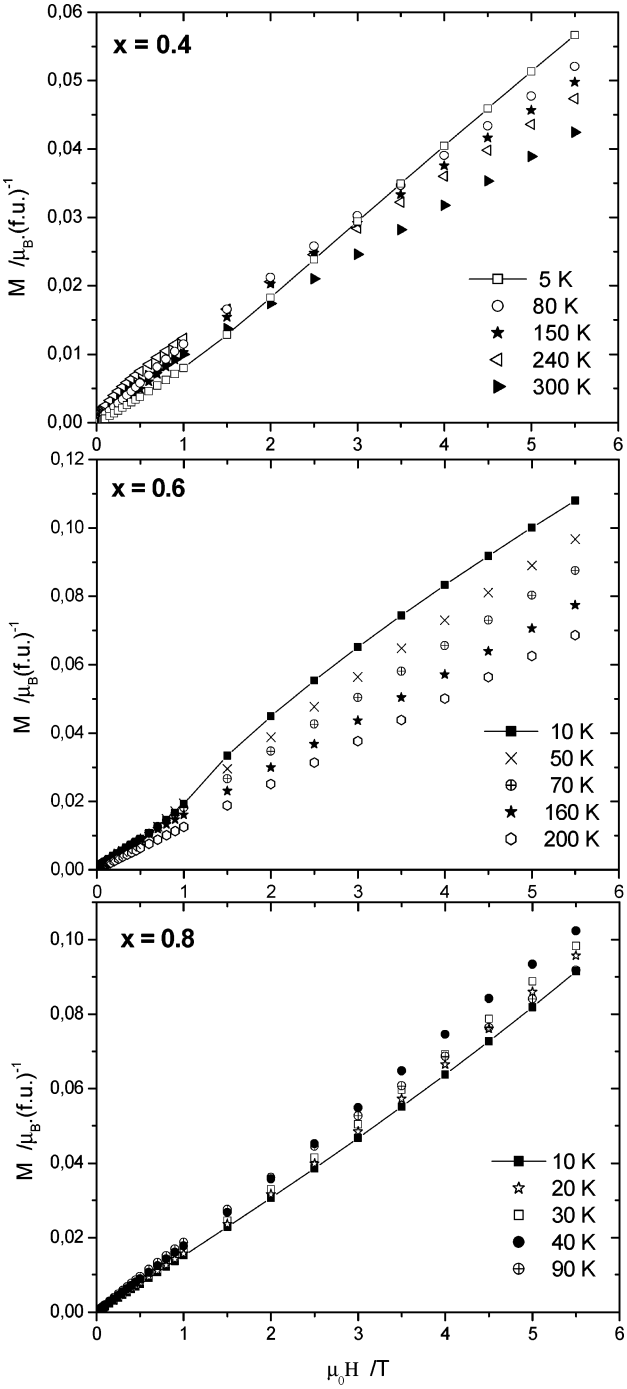

Figure 5. Magnetization as a function of the applied magnetic field collected at different temperatures for $La_{1-x}Sr_xFe_{0.8}Cr_{0.2}O_{3-\delta}$. The depicted lines are visual aids to emphasize the slope variation induced by the applied field in the M−H curves measured at the lowest temperatures.

unchanged value of magnetization between 100 and 250 K (FC curve) and a significant decrease for temperatures below 100 K.

From the analysis of the linear behavior in the inverse susceptibility versus temperature curves (insets in Figure 4), the effective magnetic moment values of 4.6(1) μ_B and 4.4(1) μ_B were extracted for the $x = 0.6$ and 0.8 samples, respectively. The fact that these values are similar indicates that the Fe/Cr valences in both samples are identical, which is consistent with the stabilization of the <Fe/Cr−O> for these two samples (Figure 2). As shown in Figure 6, where

(15) Sá, M. A. IFIMUP. Private communication, 2005.
(16) Belayachi, A.; Loudghiri, E.; El Yamani, M.; Nogues, M.; Dormann, J. L.; Taibi, M. *Ann. Chim. Sci. Mater*. **1998**, *23*, 297.
(17) Goodenough, J. B. *Magnetism and the Chemical Bond*; Interscience: New York, 1963.
(18) Battle, P. D.; Bollen, S. K.; Gibb, T. C.; Matsuo, M. *J. Solid State Chem.* **1991**, *90*, 42.

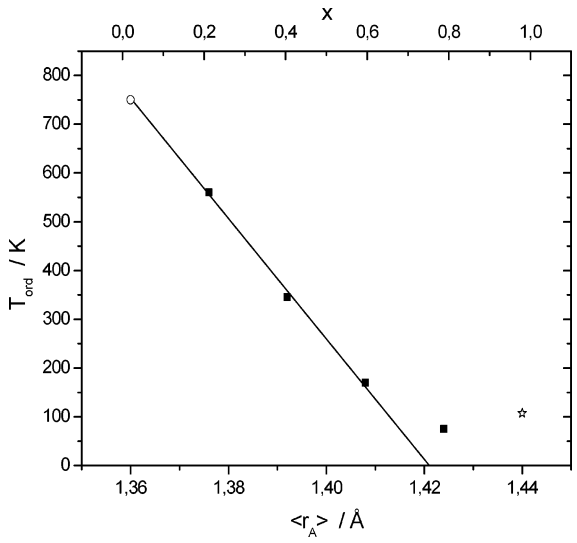

Figure 6. Magnetization ordering temperature (T_{ord}) vs cation A mean radius $<r_A>$. Closed squares, present data; open circle, data from ref 16; open star, data from ref 19. The depicted line is the linear fit to the points with $x = 0.2$, 0.4, and 0.6.

previously reported results for $LaFeO_3$[16] and $SrFeO_{2.95}$[19] were included for comparison purposes, there is a monotonic decrease of T_{ord} with the increase of $<r_A>$ (which mimics the Sr content) for $x \leq 0.6$. This trend is broken for $x \geq 0.8$, indicating that a different charge compensation mechanism appears in this case, corroborating the previous suggestion (see structural discussion) of an increased role for oxygen vacancy formation on the overall charge compensation regime. Although the bond angles for the $x = 0.8$ compound are close to 180° (Table 4), the increase of oxygen vacancies in this composition contributes to the weakening of the magnetic interactions.

Conclusions

The effect of Sr doping on the structural features and magnetic behavior of $La_{1-x}Sr_xFe_{0.8}Cr_{0.2}O_{3-\delta}$ ($x = 0.2$, 0.4, 0.6, and 0.8) phases was evaluated, with the aim of providing a better understanding of the characteristics exhibited by these materials.

As lanthanum is substituted by strontium, a structural transition is observed in the perovskite series $La_{1-x}Sr_xFe_{0.8}Cr_{0.2}O_{3-\delta}$. While the $x = 0.2$ compound exhibits an orthorhombic structure, a gradually less distorted rhombohedral symmetry is obtained for $x = 0.4$, 0.6, and 0.8, in agreement with the calculated tolerance factor values. Monotonic decreases with increasing x were found for both the <Fe/Cr−O> bond length and pseudocubic lattice parameter (a') for compositions $0.2 \leq x \leq 0.6$.

These results are consistent with an increase in the mean oxidation state of the transition metals, Fe and Cr, as the preferred charge compensation regime. The expansion of the lattice observed for the $x = 0.8$ composition and the apparent stabilization of the <Fe/Cr−O> bond length for samples $x = 0.6$ and $x = 0.8$ clearly suggest a change in the charge compensation regime toward oxygen vacancy formation.

For all samples, an overall antiparallel coupling of the magnetic moments is observed, characteristic of the Fe^{3+}−O−Fe^{3+} and Cr^{3+}−O−Cr^{3+} interactions, with the ordering temperature decreasing significantly as strontium content increases. This weakening of the antiparallel coupling is attributed to a significant number of cations in higher oxidation states. The competition between coexisting antiferromagnetic and ferromagnetic interactions leads to frustration and explains the modifications of the magnetic state detected at low temperatures. The similar magnetic moments determined for samples $x = 0.6$ and $x = 0.8$ and the fact that $x = 0.8$ breaks the trend of monotonic decrease of the ordering temperature with increasing Sr content corroborate the suggestion of a charge compensation regime change at high Sr doping.

Acknowledgment. T. Ramos acknowledges FCT, Portugal, for the postdoctoral Grant SFRH/BPD/14028/2003. The authors are grateful to M. A. Sá from the Instituto de Física dos Materiais da Universidade do Porto, for the VSM measurement. This work was supported by FCT, POCI, and cofinanced by FEDER (POCI/QUI/58915/2004).

CM060689S

(19) Zhao, Y. M.; Yang, X. J.; Zheng, Y. F.; Li, D. L.; Chen, S. Y. *Solid State Commun.* **2000**, *115*, 365.